Tunnelling and Underground Space Technology 81 (2018) 391–402

Contents lists available at ScienceDirect

Tunnelling and Underground Space Technology

journal homepage: www.elsevier.com/locate/tust

Novel rockburst criterion based on the TBM tunnel construction of the Neelum–Jhelum (NJ) hydroelectric project in Pakistan

C.S. Ma[a,b,c], W.Z. Chen[a,d,*], X.J. Tan[a], H.M. Tian[a], J.P. Yang[a], J.X. Yu[e]

[a] State Key Laboratory of Geomechanics and Geotechnical Engineering, Institute of Rock and Soil Mechanics, Chinese Academy of Sciences, Wuhan, Hubei 430071, China
[b] University of Chinese Academy of Sciences, Beijing 100049, China
[c] Patent Examination Cooperation Hubei Center of The Patent Office, SIPO, Wuhan, Hubei 430000, China
[d] Research Center of Geotechnical and Structural Engineering, Shandong University, Jinan, Shandong 250061, China
[e] School of Civil Engineering, Henan Polytechnic University, Jiaozuo, Henan 454000,China

ARTICLE INFO

Keywords:
TBM
Rockburst criterion
In situ stress
Rockmass strength
The strength-stress ratio method

ABSTRACT

The assessment of rockburst proneness has become a major technical bottleneck in brittle, and high-strength hard rock under high local stresses. Various approaches or criteria have been used over the years to predict rockburst, many of them were within an acceptable range, while some too conservative, simple and missing comprehensive consideration of rockmass quality and excavation characteristics, particularly during the tunnel construction phase. Aiming at the shortage, a novel rockburst criterion was put forward, which is defined as the ratio between the rockmass strength and the horizontal stress perpendicular to the tunnel axis as determined. First, the rockmass strength based on the Hoek–Brown strength criterion was estimated by accounting for important parameters such as rock strength, brittleness coefficient, the quantitative geological strength index (GSI), the TBM construction disturbance, and the in situ stress. Furthermore, in practical application at the NJ-TBM tunnel, the quantitative models of the geological strength index (GSI) and rock uniaxial compressive strength were proposed based on the boring/specific energy (SE) information and the field penetration index (FPI) recorded in the TBM performance database, respectively. The observations and classification of 26 rockbursts cases in different geological units indicate that the novel criterion greatly enhanced the accuracy and applicability of rockburst prediction during the construction phase, through comparative analysis with the traditional criteria.

1. Introduction

Rockburst is an instantaneous, severe as well as common geo-hazard occurring in brittle, massive and high-strength hard rock under high local stresses (Jenkins et al., 1990; Stillea and Palmströmb, 2003; Ma et al., 2015; Cai, 2016). When the mechanical state of rock was observed to be unbalanced, dynamic instability occurred in which potential energy was released in a sudden, sharp, and violent form, along with other phenomena such as slabbing, spalling, ejection, and throwing (Hedley and David, 1992; Kaiser et al., 1996, Kaiser and Cai, 2012). This catastrophic hazard has constrained the efficient and safe construction of tunnels and introduces greater threats to underground openings, equipment, and worker safety (He et al., 2015; Sousa, 2012). The assessment of rockburst proneness has become a major technical bottleneck in deep-buried tunnel construction (Ma et al., 2015) and contributions toward a better understanding of rockburst events will help develop and advance understanding of rock mechanics.

Thus far, various theories or approaches regarding rockburst prediction have been conducted, focusing on two aspects: field monitoring for real-time rockburst and theoretical analysis based on rockburst failure mechanisms.

The exact location and time of rockburst occurrences are determined using data from appropriate in-situ measurements and testing methods including the microgravity method, the photo-elastic method, the convergence measurements method, the drilling-yield method, and the acoustic emission and microseismic techniques, among others (Chen et al., 2015; Ma et al., 2015). However, monitoring approaches for rockbursts have often been of limited application, due to the expensive and immature nature of the technology caused by the complexity of rockmass and various environmental factors in deep-buried tunnels.

Theoretical analysis based on the rockburst failure mechanism consist of strength, stiffness, energy, instability and fractal theory et al. The corresponding single strength-stress ratio index or stress-strength

* Corresponding author at: State Key Laboratory of Geomechanics and Geotechnical Engineering, Institute of Rock and Soil Mechanics, Chinese Academy of Sciences, Wuhan, Hubei 430071, China.
E-mail address: wzchen_SDU@163.com (W.Z. Chen).

https://doi.org/10.1016/j.tust.2018.06.032
Received 16 June 2017; Received in revised form 20 July 2017; Accepted 28 June 2018

Table 1
The corresponding rockburst criteria and classification items.

Multiple discriminant criteria	Reference	Formula	Rockburst grade			
			No	Light	Moderate	Intensive
The strength-stress ratio index or stress-strength ratio index	Barton et al. (1974)	σ_{ci}/σ_1	> 10.00	10.00–5.00	5.00–2.50	< 2.50
	Russenes (1974)	$\sigma_{\theta\,max}/\sigma_{ci}$	≤0.20	0.20–0.30	0.30–0.55	≥0.55
	Hoek and Brown (1980)		0.34 Minor spalling	0.42 Severe spalling	0.56 Heavy support	0.70 Severe rockburst
	Turchaninov (1978)	$(\sigma_{\theta\,max} + \sigma_L)/\sigma_{ci}$	≤0.30	0.30–0.50	0.50–0.80	≥0.80
	Code for geological survey of water resources and hydropower projects (2008)	σ_{ci}/σ_{max}	> 7.00	4.00–7.00	2.00–4.00	< 2.00
	Zhang et al. (2012)	σ_1/σ_{ci}	≤0.15	0.15–0.20	0.20–0.40	≥0.40
The burst energy coefficient	Goodman (1980)	$R = W_E/W_P$	> 1 (Having the rockburst tendency)			
The strain energy storage coefficient	Kidybiski (1981)	$F = W_{st}/W_{sp}$	≤2.00	2.00–5.00		≥5.00
The brittleness coefficient of rocks	Zhang et al. (2012)	$B = \sigma_{ci}/\sigma_t$	< 15.0	15.0–18.0	18.0–22.0	> 22.0
The integrality modulus		K_v	< 0.55	0.55–0.60	0.60–0.80	> 0.80

Note: σ_{ci} is uniaxial compressive strength; σ_1 is maximum principal stress of in situ stress; $\sigma_{\theta\,max}$ is maximum tangential stress of cross section in disturbed zone; σ_L is radial stress of cross section in disturbed zone; σ_{max} is the maximum horizontal stress perpendicular to the tunnel alignment; σ_1, $\sigma_{max} < \sigma_{\theta\,max}$. W_E is the elastic strain energy accumulated before rock failure; W_P is the elastic strain energy accumulated.W_{sp} represents the spent energy by plastic deformation during unloading process. W_{st} represents the stored energy in the rocks.σ_t is the tensile strength.

ratio index (Barton et al., 1974; Russenes, 1974; Turchaninov, 1978; Hoek and Brown, 1980;Code for geological survey of water resources and hydropower projects, 2008; Zhang et al., 2012), the rockmass integrality modulus K_v, the brittleness coefficient of rocks B (Zhang et al., 2012), the strain energy storage coefficient F (Kidybiski, 1981) and the burst energy coefficient R (Goodman, 1980) have been proposed and widely applied in practice as long-term preliminary or regional prediction of rockburst tendencies during the exploration phase. The corresponding rockburst criteria and classification items were listed in Table 1.

However, widely used, due to the complexity of rockmass and various excavation characteristics, single rockburst criteria have been found to have some limitations in accuracy and reliability. Take the most common strength-stress ratio index for example, uniaxial rock strength and in situ stress are considered simply, and rockmass quality and excavation characteristics are ignored, resulting in the predicted deviations when evaluating the character of rockbursts.

With the advancements in the understanding of rockburst mechanism, taking into consideration the limitations of the single index criteria, scholars have gradually begun to apply multi-index comprehensive criteria to predict rockburst(Gu, 2001; Zhang et al., 2012;Shang et al., 2013). The relationships depicted in the evaluation indexes are basically conjunctive “and-type” relationships, rarely classified as ”or-type“. Because a rockburst does not represent a clear-cut system due to many uncertainties, a wide range of prediction methods are required, classifying the factors affecting rockburst occurrences as random, fuzzy, matter–element analysis theory, or even both (Adoko et al., 2013; Wang et al., 2015). While the influence factors of rockburst are considered more comprehensively with parallel multi-index comprehensive criteria, it is noted that the validity of existing random or fuzzy models, to some extent, depends upon the subjective understanding of the researchers. Additionally, some parallel multi-index criteria are only applicable to long-term or regional predictions during the design phase. These criteria are limited in applicability and reliability, particularly during the construction phase.

The occurrence of rockburst is closely related to the characteristics of rockmass, in situ stress, geologic structure, and excavation disturbance. Various approaches or criteria have been used over the years to predict rockburst, while some too conservative, simple and missing comprehensive consideration of rockmass quality and excavation characteristics, particularly during the tunnel construction phase. This paper aims to address the above shortage mentioned by taking into consideration the multiple factors present during the tunnel construction phase, and establish a novel criterion to evaluate the rockburst tendency accurately.

In this paper, first, based on the details of geological settings, as well as the in situ and laboratory tests, the detailed statistical analysis of rockburst characteristics and the limitations of traditional criteria are summarized. Then, a novel rockburst criterion is presented using the strength-stress ratio, which is defined as the ratio between the rockmass strength σ'_{rm} and the maximum horizontal stress perpendicular to the tunnel axis σ_{max}. The rockmass strength, based on the Hoek–Brown strength criterion, replaces the uniaxial compressive strength σ_{ci} by accounting for important parameters such as the rock strength σ_{ci}, the brittleness coefficient σ_{ci}/σ_t, the quantitative GSI, the excavation disturbance factor D, and the minor principal stress σ'_3. Furthermore, in practical application at the NJ-TBM tunnel, the quantitative models of the geological strength index (GSI) and rock uniaxial compressive strength (σ_{ci}) were proposed based on the boring/specific energy (SE) information and the field penetration index (FPI) recorded in the TBM performance database, respectively. Based on the rockburst database consisting of 26 observations and classification at the NJ-TBM tunnel, the applicability and reliability of the novel rockburst criterion is verified through comparative analysis with the traditional rockburst criteria in the end.

2. The TBM tunnel of the Neelum–Jhelum hydroelectric project (NJ-TBM tunnel)

2.1. Project description and geotechnical conditions

The Neelum–Jhelum Hydroelectric Project is located in the Muzaffarabad district of Azad Jammu Kashmir (AJK), Pakistan (shown in Fig. 1). Just over 11 km of the twin tunnel system will be excavated by TBM, while the remainder will be excavated by drill-and-blast. The maximum depth of the tunnels is nearly 2000 m. In the tunnel areas under deep cover, the rockmass is generally very tight and no large inflows or groundwater pressures have been encountered. Therefore, the rockmass will be considered dry.

The project is located in the Himalayas, a geologically young mountain range of spectacular height that developed as a result of the collision between various continental and micro continental plate fragments during the late Mesozoic to late Cenozoic periods. The main geological formation outcropped is the Murree Formation, except at the tunnel intake, which is partly in igneous or metamorphic rocks belonging to the Panjal Formation.

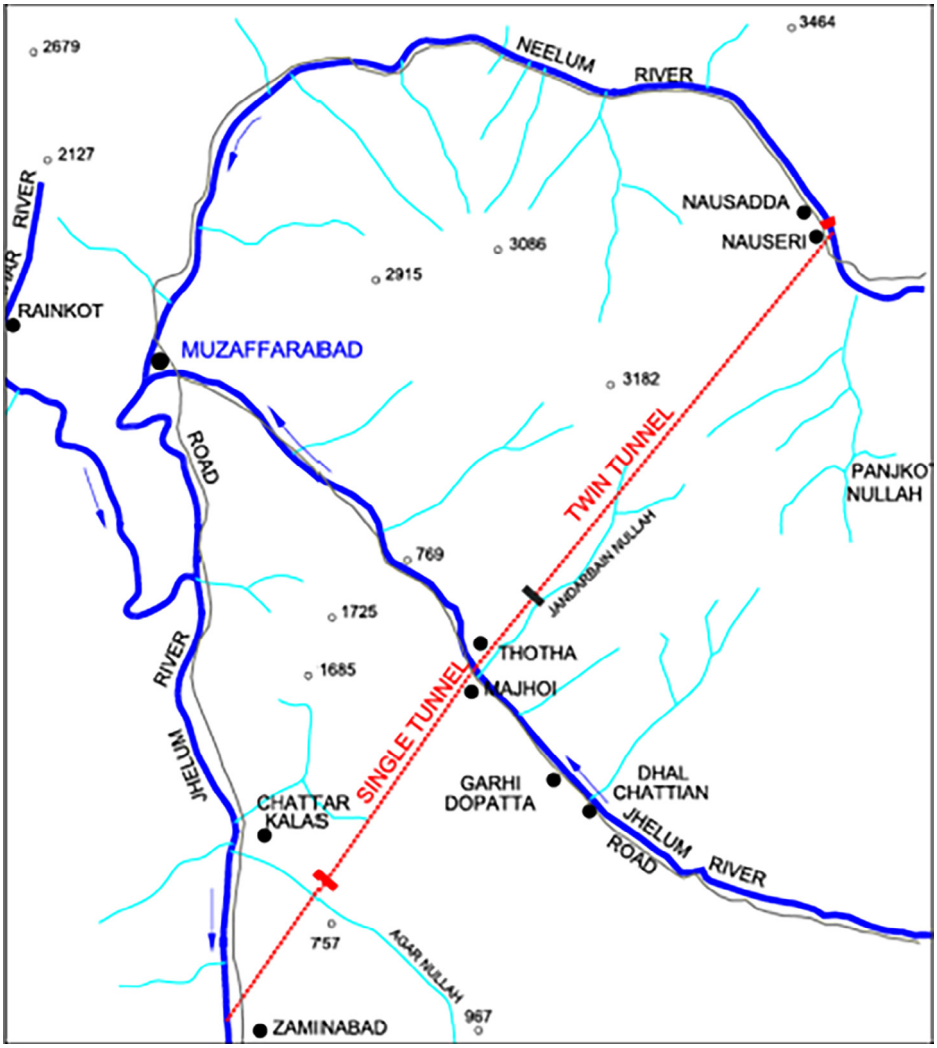

Fig. 1. The headrace tunnel scheme of Neelum-Jhelum hydroelectric project.

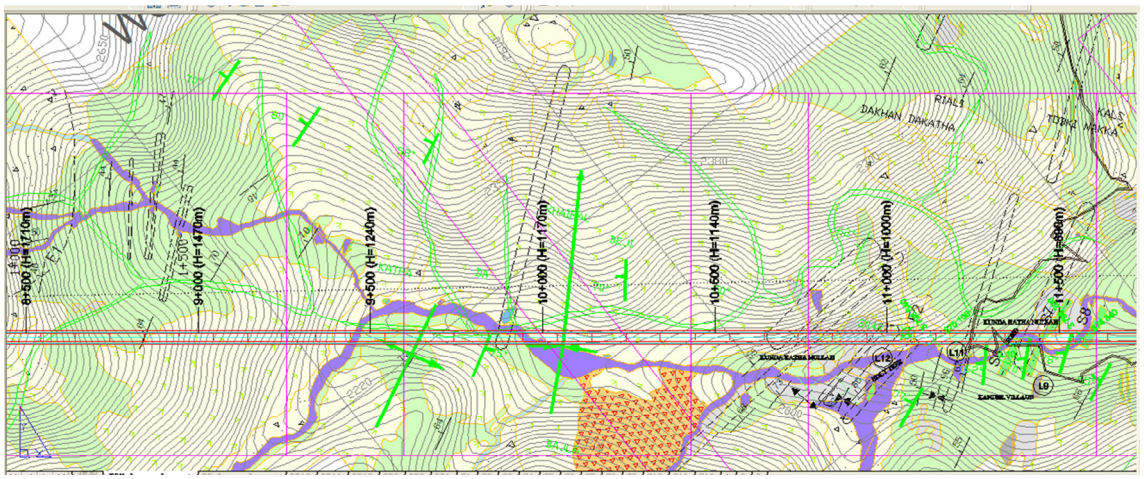

Fig. 2. Structural geology along the tunnel.

Structurally, the area around the TBM tunnel is moderately folded and gently faulted. As shown in Fig. 2, the tunnel in the bored section has passed through some closed light synclines and anticlines, and a fold stroke in NW300°–330°. In most areas, the bedding was observed to be steeply dipping and striking almost perpendicular to the bearing of the tunnel alignment (normal condition). Local folding driven disturbance to this dominant structure appears fairly common. Fault structures caused bedding dips to flatten and to be folded into a drag fold with a thickened fold hinge against the fault. This feature leads to tremendous rockburst hazards.

The Murree Formation at the location of the TBM tunnels consists of alternating beds of grey medium to fine grained sandstone and reddish

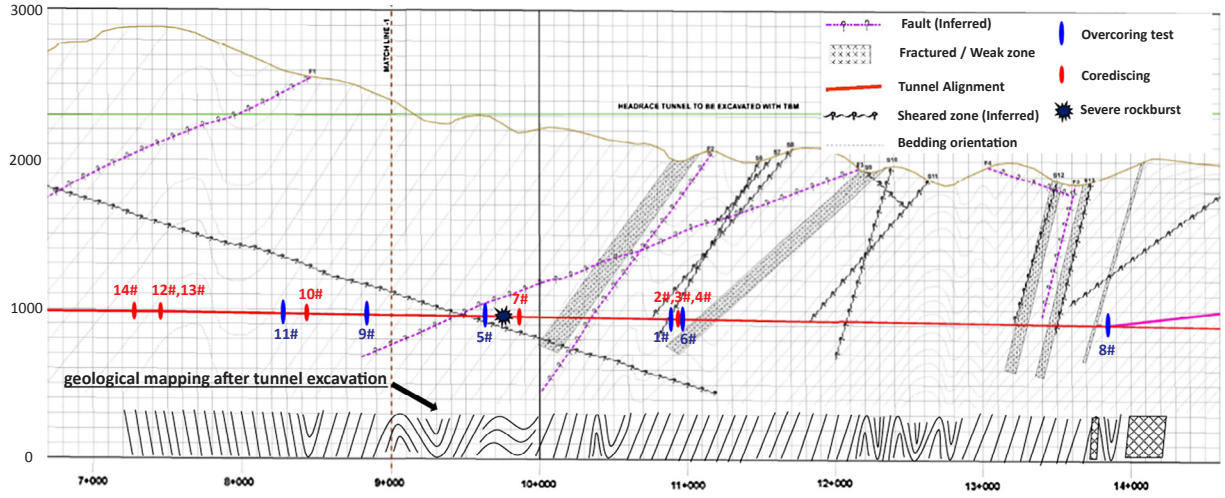

Fig. 3. Geological mapping and stress measurement locations.

colored fine to very fine grained siltstone with occasional thin mudstone layers. Thick sandstone beds are often very massive and competent. A number of intact rock material test campaigns have been conducted over the life of the project. The summary of intact rock properties were derived from a review of available rock testing data.

During excavation at the NJ-TBM tunnel, a number of light, several moderate, and rare intensive rockbursts occurred. Detailed observation of rockbursts had been documented during excavation, and these observations were used as the database for this study.

2.2. Field investigation of in situ stress

2.2.1. Description of in situ tests and results

During the construction stage, the improved over-coring technique tests and confining-pressure experiments were carried out. The testing locations are approximately 15 m off the tunnel wall to ensure that the disturbance from the construction will not affect the in situ stress field. The locations of testing boreholes, corediscing records and geological map after tunnel excavation are plotted in Fig. 3.

The magnitude, orientation, and dip angle of 3D geo-stresses are derived and are presented in Table 2. To compare the results from different test locations, it is best to transform the principal stress components to the common tunnel coordinate system. The stress tensor are derived through coordinate transformations, as also given in Table 2.

The test results show that the maximum compressive stresses reach 50–116 MPa. It is found that for the maximum compressive stresses, the trends are among 270–340° and dips −30° to 30° from the horizontal plane. The results show that the horizontal tectonic stress field dominates in this area.

2.2.2. Analysis of the test results

The distribution law of the in-situ stress field evinces the following characteristics:

(1) Considering the inherent heterogeneity of rock mass, stresses measured at different locations could be different with each other, even at the same borehole. It is more reasonable to remove the conspicuously unconventional test results (region of stress concentration). Fig. 4 show the values of σ_X, σ_Y, σ_Z from the common tunnel coordinate system increase almost linearly with burial depth. Mathematical relationships with the burial depth are derived as follows:

$$\sigma_X = 0.0273H + 16.807 \quad (1)$$

$$\sigma_Y = 0.0341H + 4. .423 \quad (2)$$

$$\sigma_Z = 0.0337H - 0.3687 \quad (3)$$

where H represents the depth of cover in the location of the test, in units of m. Note that the correlation coefficients between the three stresses and the depth are 0.671, 0.812 and 0.83, respectively. It is noted that σ_X

Table 2
Test results using with CSIRO hollow inclusion strain gauge method.

No.	Depth (m)	σ_1			σ_2			σ_3			σ_X	σ_Y	σ_Z
		Mag (MPa)	Dip (°)	Brg (°)	Mag (MPa)	Dip(°)	Brg (°)	Mag (MPa)	Dip (°)	Brg (°)	MPa	MPa	MPa
1	1040	73.9	6	327	37.7	37	242	26	52	50	71.3	38.6	32.3
2	1040	108.8	11	330	35.2	47	228	23.7	41	69	95.1	39.9	32.7
3	1040	82.1	13	339	37.7	62	224	25.8	25	75	65.3	42.9	37.5
4	1200	88.9	2	297	54.9	60	203	11.7	30	29	86.9	24.4	44.2
5	1010	102.9	33	292	40.6	14	193	25.1	54	84	78.9	41.4	48.3
6	1010	107.3	21	338	40.9	64	119	32.7	13	243	82.7	49	49.3
7	1010	102.9	32	312	48.4	47	195	24.4	37	70	89.8	43.8	45.7
8	800	50.7	14	102	24.3	43	206	19.5	44	358	43.4	27.6	23.5
9	800	54.9	30	107	27.7	13	204	21.2	57	315	43.5	30.6	29.7
10	800	50.7	39	101	21.3	22	210	15.9	43	322	32.7	24.8	30.4
11	1530	53.4	14	70	51.7	5	339	43.2	75	227	52.4	52	43.9
12	1530	50.6	7	102	48.5	13	10	40.7	75	221	49.9	48.6	41.3
13	1530	60.7	2	95	56.4	3	5	47.6	86	211	59.5	57.5	47.7
14	1785	109.2	20	269	67.2	60	36	4.7	22	170	59.5	59	62.6
15	1785	116.8	35	282	75.8	29	35	36.2	42	155	82	76.1	70.7

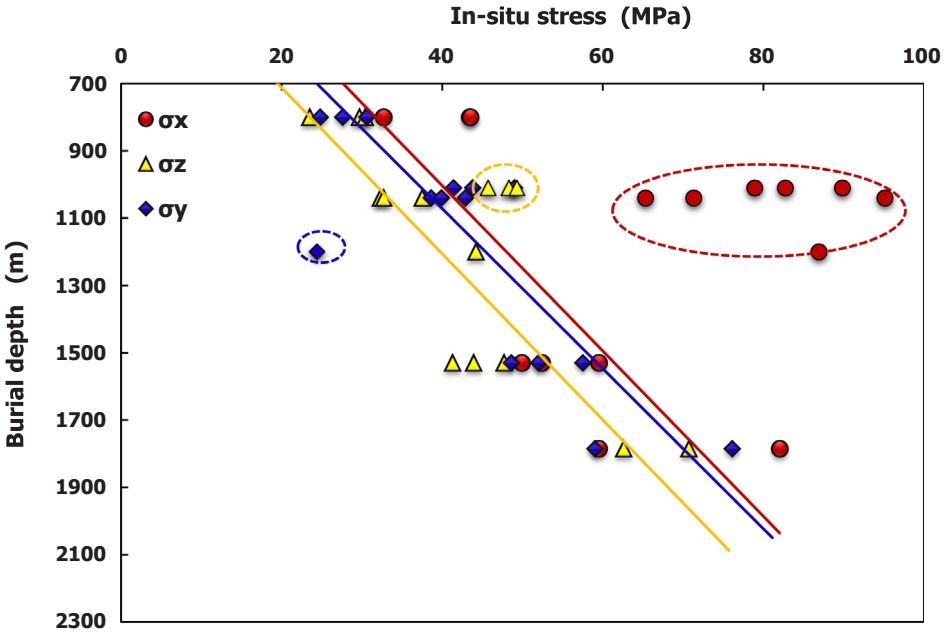

Fig. 4. Regression analysis of the in-situ stresses with burial depth.

equals the maximum horizontal stress perpendicular to the tunnel alignment σ_{max}, and the vertical stress σ_Z equals the minimum principle stress approximately. These equations will be used to obtain the in-situ stress in the places where no in situ tests are available.

(2) The fitting coefficient 0.0337 of vertical stress means an increment of 100 m depth causes an increment of 3.37 MPa of vertical stress. It is larger than 2.7 MPa, i.e. the theoretical vertical stress. The result is consistent with the hydraulic test results obtained in the feasibility study of the NJ-TBM project, which all the values were found to vary between 150% and 85% of the theoretical gravitational stress (Khan, 2012).
(3) These results of $1.1 < \sigma_X/\sigma_Z < 2.9$, with an average of 1.6 indicated that the in-situ stress field was dominated by the horizontal tectonic stress, which are all compressive stresses that approximately coincide with the results of the regional tectonic analysis.

3. Statistics of rockburst events and limitations of the traditional rockburst criteria

3.1. Statistics of rockburst events

During excavation at the NJ-TBM tunnel, a number of light, several moderate, and rare intensive rockbursts occurred. Fig. 5 shows the distribution of rockburst events in the TBM tunnel along with burial depth and measured in situ stress. According to the detailed in situ statistical analysis, the following rockburst characteristics can be summarized:

(1) Within the 6.6 km between chainages 13 + 500 and 06 + 900, rockburst frequencies increase then decrease as the burial depth increases. Two intensive rockburst events took place at a shallow depth (below 800 m depth), while several light or moderate rockbursts occurred at the maximum overburden depth in the 1700–1950 m range, although the maximum principal stress was as high as 116 MPa. This suggests uncertainty as to whether higher in situ stresses will lead to more severe rockbursts.
(2) It is worth noting that the occurrence of intensive rockbursts is highly correlated with the character of the rockmass and geologic structures. Fig. 6 shows the typical rockburst notch of the "5.31" event, an extremely intensive rockburst that occurred between chainage 09 + 700 and 09 + 800 at a 1200 m burial depth. The surrounding rockmasses for the extremely intensive "5.31" rockburst mainly consist of intercalated thick-bedded sandstone and grained siltstone, which is brittle and high in strength. Geologic structure analysis demonstrated that fault structures caused bedding dips to flatten and to be folded into a drag fold, as shown in Fig. 7 (Bawden, 2015). Higher in situ stress (about 87 MPa) and local fault driven disturbances led to the "5.31" rockburst event. Notably, before the tremendous rockburst event, several light or moderate rockbursts occurred. Several other remarkably intensive rockburst events have been recorded when encountering similar local tectonic geological conditions.

3.2. Limitations of the traditional rockburst criterion

The traditional strength-stress ratio criteria are widely used for rockburst classification and prediction, e.g., Barton et al. (1974), Russenes (1974) and Zhang et al. (2012). Using the NJ-TBM tunnel as an example, the threshold ratio for the criteria and corresponding intensity are summarized in Table 3.

Classification for the actual rockburst cases were assessed in discordance with the three criteria. The tunnel was under moderate to intensive rockburst risk with the traditional strength-stress ratio criteria. While most actual rockbursts were light; only several moderate rocskbursts and the rare intensive rockbursts occurred during tunnel excavation (Fig. 5). Some light and several moderate rockbursts occurred at the maximum overburden depth of 1700–1950 m, in spite of the higher stress as high as 120 MPa. The "5.31" rockburst case illustrates that the occurrence of intensive rockburst is also highly correlated with higher in situ stress, complex rockmass properties, and geologic structures (Fig. 7).

The traditional rockburst criterion is convenient for design engineers to understand and apply this criterion, but it is considered too conservative and simple to predict rockburst events in complex geological conditions. While the influence factors of rockburst are considered more comprehensively with parallel multi-index comprehensive criteria, it is noted that the validity of existing models, to some extent, depends upon the subjective understanding of the researchers, and are limited in applicability and reliability, particularly during the

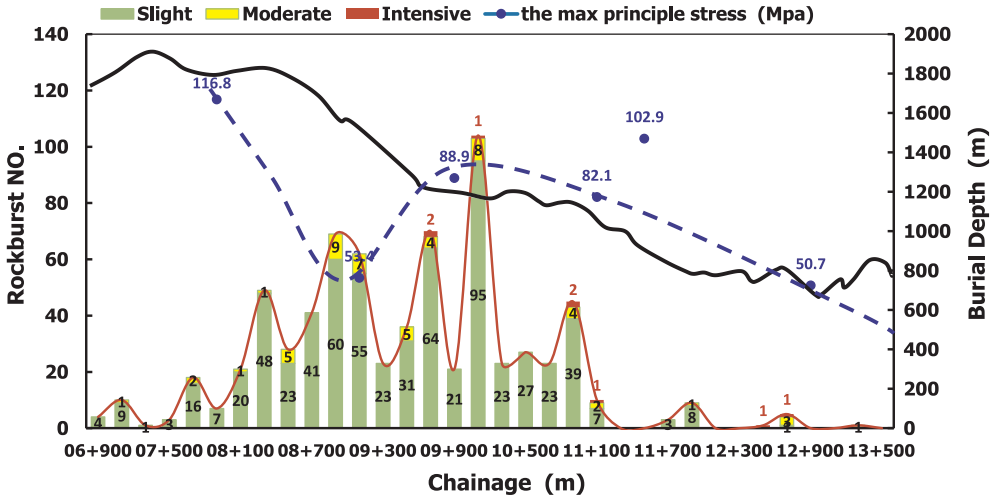

Fig. 5. Rockburst events with burial depth of the tunnel and in-situ stress.

construction phase. In addition, rockmass quality and construction characteristics are also ignored in the traditional rockburst criterion. It is essential to establish an appropriate criterion to evaluate the rockburst tendency accurately with the consideration of rockmass quality and construction characteristics during the construction phase.

4. Development of the novel rockburst criterion based on the rockmass strength and in situ stress

4.1. The novel rockburst criterion

The strength-stress ratio is often used for rockburst evaluation by most international scholars, which can take key influencing factors of rockburst into account. Therefore, the novel rockburst criterion is still based on this idea. The rockburst occurred generally due to the immediate unloading of surrounding rockmass from the triaxial condition. While the uniaxial compressive strength of traditional rockburst criterion is not representative of rockmass quality and construction characteristics. Therefore, the rockmass strength under a certain confined pressure is estimated to replace the uniaxial compressive strength σ_{ci}, addressing the limitations of previous methods.

The main method for estimating the rockmass strength is based on strength theory, using the index of rockmass classification (RMR, GSI, Q, et al.) combined with partial rock mechanics test indexes. The rockmass strength based on the Hoek–Brown strength criterion is widely applied and recognized (Hoek and Brown, 1997; Hoek et al., 1998, 2002; Marinos and Hoek, 2000). By introducing the parameters of stress state, rock strength, geologic structure, and construction

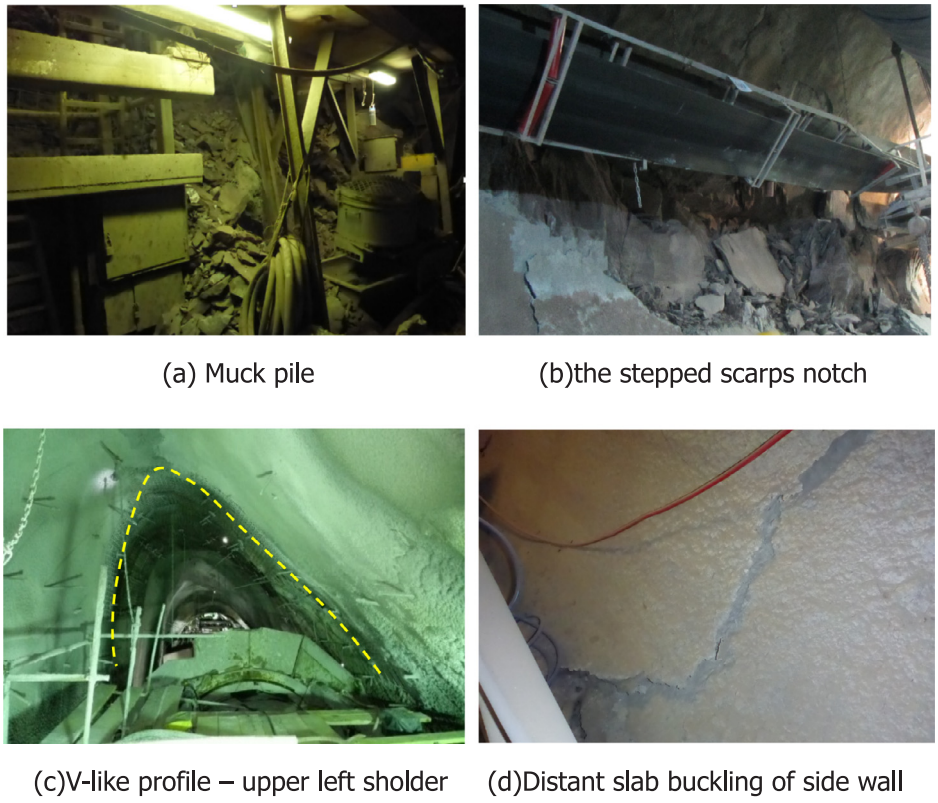

Fig. 6. The rockburst damage conditions.

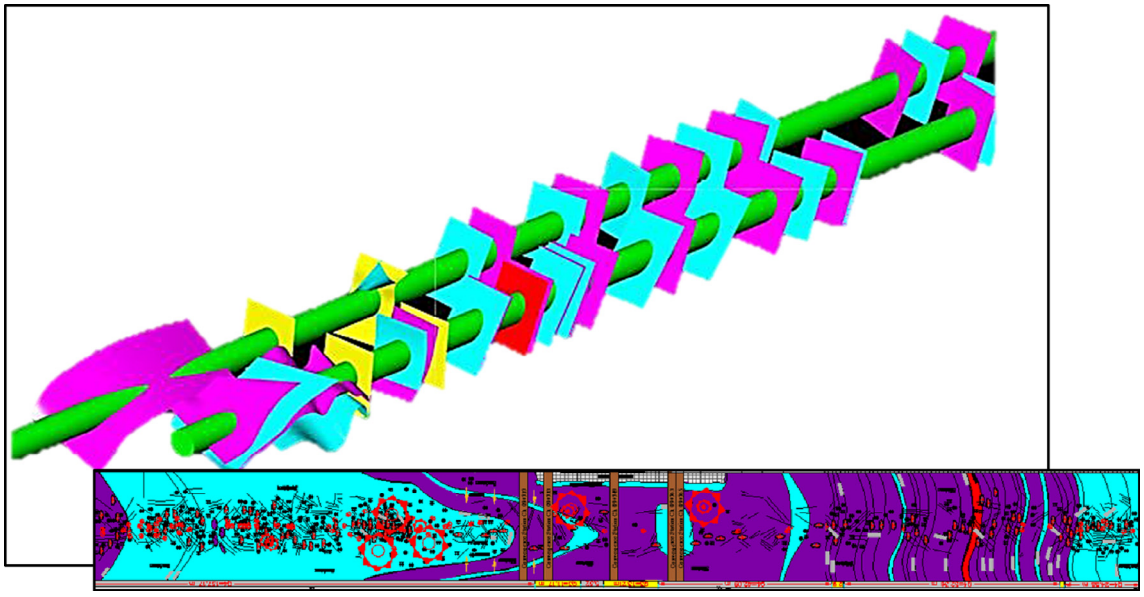

Fig. 7. Local folding with bedding- an apparent structural anomaly (Bawden, 2015).

disturbance, the rockmass strength estimation formula derived from Hoek–Brown strength criterion can be summarized as follows:

$$\sigma'_{rm} = \sigma'_3 + \sigma_{ci}\left(m_b\frac{\sigma'_3}{\sigma_{ci}} + s\right)^{\alpha} \tag{4}$$

where σ'_{rm} is the triaxial rockmass strength based on the Hoek–Brown strength criterion, σ_{ci} is the uniaxial compressive strength of the intact rock material, and σ'_3 is the minimum principal stress at failure.

m_b is a reduced value of the material constant m_i and is given by:

$$m_b = m_i \exp\left(\frac{GSI-100}{28-14D}\right) \tag{5}$$

$$m_i = \frac{\sigma_{ci}}{\sigma_t} \tag{6}$$

where σ_t is the uniaxial tension strength.

Components s and α are constants for the rockmass given by the following relationships:

$$s = \exp\left(\frac{GSI-100}{9-3D}\right) \tag{7}$$

$$\alpha = 0.5 + \frac{1}{6}\left(e^{-GSI/15} - e^{-20/3}\right) \tag{8}$$

where GSI is the geological strength index; D is an excavation disturbance factor varying from 0 for undisturbed in situ rockmass to 1 for very disturbed rockmass. Undisturbed rock mass conditions with D = 0 achieved by TBM excavation are discussed in guidelines for the selection of D (Hoek et al., 2002).

Ultimately, the novel rockburst criterion is proposed based on the rockmass strength-stress ratio:

$$RPI\ (\text{Rockburst Proneness Index}) = \frac{\sigma'_{rm}}{\sigma_{max}} \tag{9}$$

Where σ_{max} is the maximum horizontal stress perpendicular to the tunnel alignment.

Practical experience indicates that the maximum in situ stress when the surrounding rockmass failure occurs, can be expressed simply:

$$\sigma'_1 = \eta\sigma_{max} \tag{10}$$

where η is the factor of stress concentration.

According to in situ stress-state evaluations gathered from practical experience, a conclusion can be drawn that the ratio of the rock mass strength σ'_{rm} under the limiting equilibrium stress state to the maximum in situ stress σ'_1 should be less than 0.5 (Wang et al., 2009, 2011), Therefore, when $\sigma'_{rm}/\sigma'_1 = \sigma'_{rm}/(\eta\sigma_{max}) < 0.5$(also stated as $\sigma'_{rm}/\sigma_{max} < 0.5\eta$), the rockmass can be considered to be under high stress, which has a large influence on rockmass stability.

Taking a circular tunnel as an example, generally speaking, the stress concentration factor η is between 2 and 4, so when $1 \leqslant \sigma'_{rm}/\sigma_{max} \leqslant 2$, the rockmass is under high stress and in a "Intensive" rockburst state. When $\sigma'_{rm}/\sigma_{max} > 4$, obvious stress-induced damage will not occur because regions in which η is greater than 8 are rare,

Table 3
The statistics of threshold ratio for the criteria and corresponding intensity.

Chainage (m)	Depth (m)	σ_1	σ_3	Barton et al.(1974)		Russenes (1974)		Zhang et al. (2012)		Site records of rockburs
				σ_{ci}/σ_1	Result	$\sigma_\theta/\sigma_{ci}$	Result	σ_1/σ_{ci}	Result	
13 + 834	800	52.2	43.8	2.74	Moderate	0.62	Intensive	0.36	Moderate	1 OB, 1.5 m * 7 m
10 + 935	1010	104.4	27.4	1.37	Intensive	1.57	Intensive	0.73	Intensive	2 intensive, 4 light RB, crown; OB, 30 m * 6 m
10 + 881	1040	88.3	25.2	1.62	Intensive	1.31	Intensive	0.62	Intensive	1 light RB, crown; OB, 7 m * 6 m
9 + 861	1200	88.9	11.7	1.61	Intensive	1.40	Intensive	0.62	Intensive	1 intensive, 21 light RB, crown; Lots of OB
8 + 827	1500	54.9	43.8	2.61	Moderate	0.66	Intensive	0.38	Moderate	1 moderate, 20 light RB;1 OB, 15 m * 7.5 m
8 + 422	1700	113	36.2	1.27	Intensive	1.66	Intensive	0.79	Intensive	1 moderate, 8 light RB;1 OB, 3m * 1 m
8 + 287	1785	113	36.2	1.27	Intensive	1.66	Intensive	0.79	Intensive	7 light RB; 3 small OB
7 + 440	1950	126.1	65.3	1.13	Intensive	1.71	Intensive	0.88	Intensive	3 light RB; 4 small OB
7 + 280	1860	120.2	62.3	1.19	Intensive	1.64	Intensive	0.84	Intensive	1 light RB

Note: RB and OB are the abbreviations of rockburst and overbreak.

Table 4
Threshold values for the rockburst evaluation index.

Engineering rockmass strength-stress ratio	Rockburst grade			
	Intensive	Moderate	Light	No
$\sigma'_{rm}/\sigma_{max}$	1–2	2–4	4–7	> 7

which is considered to be in a low stress state with a corresponding "light" rockburst risk. For very low stress states, a value of η around 12–20 indicates that rockmass failure does not occurs with a corresponding "no" rockburst risk. Accordingly, the Water Resources and Hydropower Projects Criteria in China considers there to be no risk of rockburst when $\sigma'_{rm}/\sigma_{max} > 7$. The final threshold values for the rockburst evaluation index are shown in Table 4.

4.2. Proper selection of rockburst influencing factors

In practical applications such as the NJ-TBM tunnel, the important parameters for predicting rockburst (the geological strength GSI, and the rock strength σ_{ci}) were obtained as follows:

- Considering the narrow space for observation in the TBM tunnel, the quantitative GSI equation was estimated by a regression analyses using TBM performance parameters.
- An empirical equation for σ_{ci} was developed based on TBM performance parameters, making a quick and accurate determination of the rock strength during construction.

4.2.1. The quantitative GSI model based on TBM parameters

The quantitative GSI value can generally be obtained based on the structure rating (SR) and surface condition rating (SCR) (Marinos et al, 2005). In this study, the relationships between different TBM performance parameters (such as Torque (M), Thrust (F), Revolutions Per Minute (RPM), Penetration (P), the field penetration index (FPI) and boring/specific energy (SE)) and the geological strength index (GSI) were investigated. Graphs (a) to (d) of Fig. 8 show the relationship between different TBM performance parameters and GSI. Table 5 lists

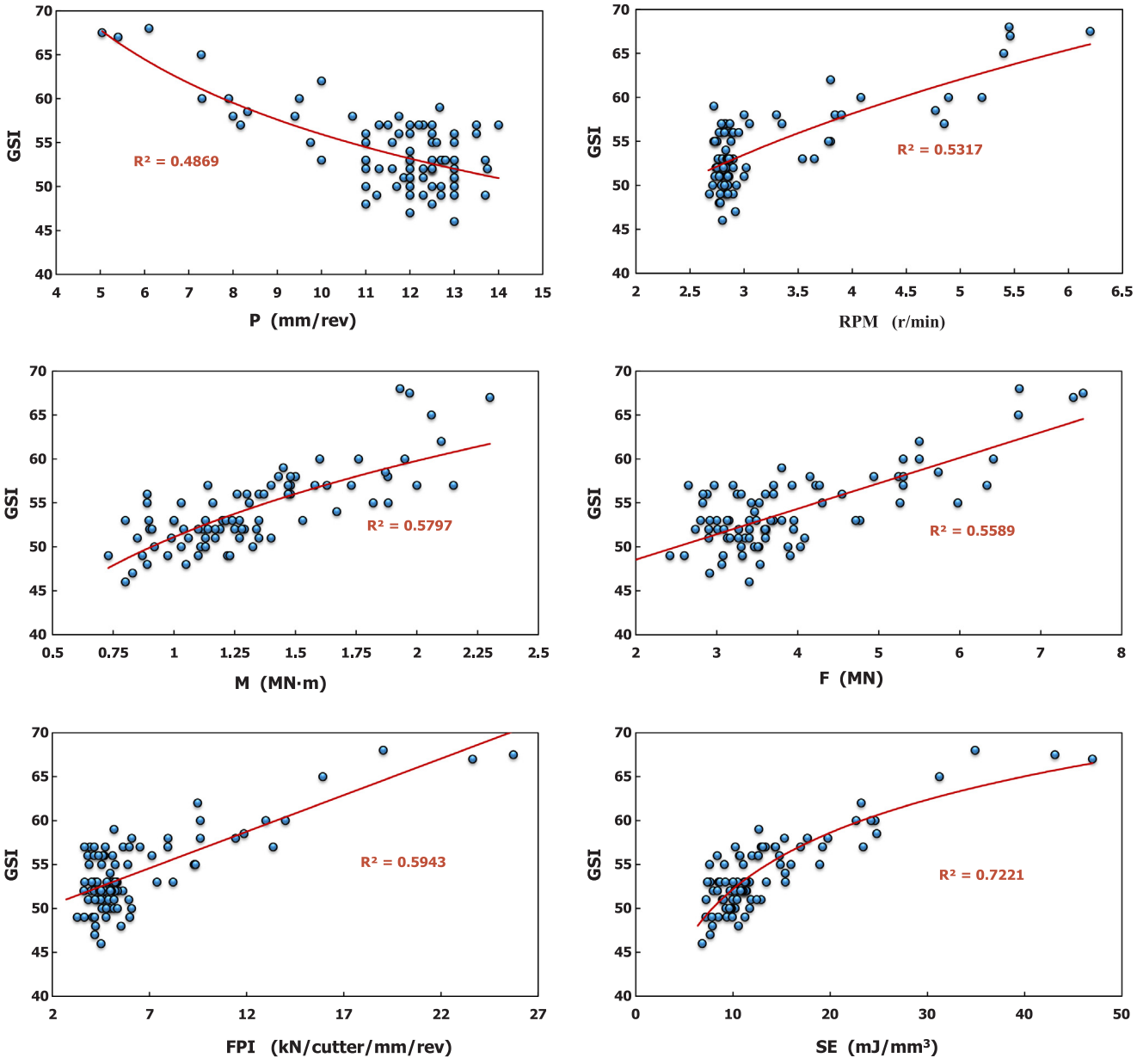

Fig. 8. Correlation between GSI and T, P, F, RPM, SE and FPI.

Table 5
Summary results of correlation of GSI with TBM parameters.

Parameter		R^2	Regression type	Relationship	Eq. no.
Simple parameters	Penetration	0.4869	Power	$GSI = 106.06 \times P^{-0.278}$	(11)
	RPM	0.5317	Power	$GSI = 38.84 \times RPM^{0.291}$	(12)
	Thrust	0.5589	Linear	$GSI = 2.9 \times F + 42.73$	(13)
	Torque	0.5797	Power	$GSI = 51.11 \times M^{0.226}$	(14)
Composite parameters	FPI	0.5943	Linear	$GSI = 0.831 \times FPI + 48.76$	(15)
	SE	0.7221	Logarithmic	$GSI = 9.26 \times Ln(SE) + 30.87$	(16)

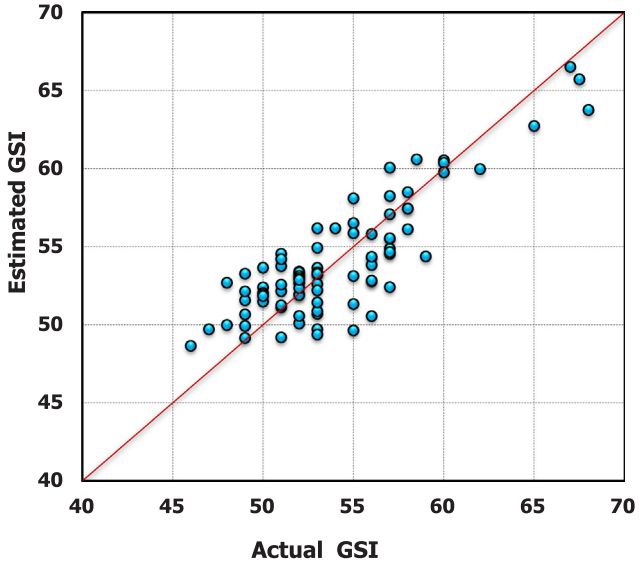

Fig. 9. Comparative analysis of two different GSI accessor method.

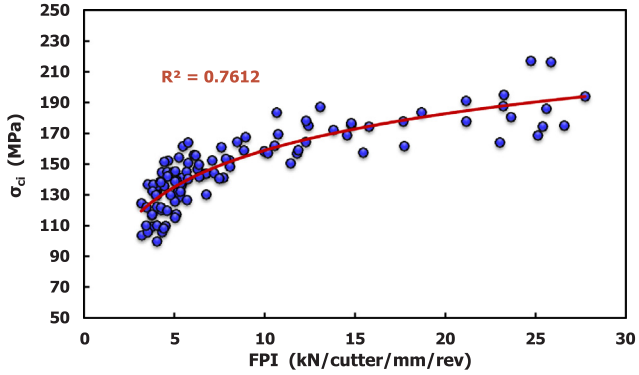

Fig. 10. Correlation between σ_{ci} and FPI.

the summary results of correlation.

As shown, the composite TBM parameters FPI and SE show better correlation than the simple parameters. Correlation results between GSI and TBM performance parameters show that R^2: SE > FPI > Torque (T) > Thrust(F) > Revolutions Per Minute(RPM) > Penetration(P). Therefore, SE was selected as a suitable parameter for developing empirical relationships between TBM parameters and GSI.

To establish these correlations, comparative analysis using two different GSI methods were carried out to verify the accuracy of GSI values based on the TBM SE parameter. The variations of absolute errors E (%) were calculated according to following formula:

$$E(\%) = \left|\frac{ActualGSI - EstimatedGSI}{ActualGSI}\right| \cdot 100 \quad (17)$$

The GSI estimated from the TBM SE parameter is compared with the observed GSI for the selected tunnel sections (Fig. 9). As shown, most ΔGSI values are less than 5. Values for E (%) are in the range of 0.01–10%, which indicates that the use of the TBM boring/specific energy (SE) parameter is an effective method for determining the value of GSI.

4.2.2. Development of the new σ_{ci} prediction model

The rock strength σ_{ci} is served as a significant mechanical parameter for accident assessment of rockburst classification. Unlike conventional drilling and blasting methods, one of the drawbacks of the use of TBMs is that the construction method prevents the direct observation of the tunnel face. Because TBMs simultaneously excavate the entire face of the tunnel as they advance, fast and accurate determination of the rock strength at the advancing face is virtually impossible. The establishment of a rapid prediction model for σ_{ci} based on TBM performance is a pressing challenge for rockmass strength estimation in TBM applications.

Some cases indicated σ_{ci} values correlate significantly with TBM parameters, and results demonstrated that FPI and σ_{ci} were positive correlation(Nelson et al., 1983; Sanio 1985; Hamidi et al., 2010; Hassanpour et al., 2009, Hassanpour et al., 2011). Therefore, in this study, regression analyses were performed between UCS and TBM performance parameters, and FPI was also selected as the most suitable machine parameter for developing empirical relationships with σ_{ci}. Fig. 10 show the correlation between σ_{ci} and the field penetration index (FPI) of TBM parameters. Logarithmic regression equation was derived as follows:

$$\sigma_{ci} = 34.35Ln(FPI) + 79.81 \quad (18)$$

This equation will be used to obtain the fast and accurate determination of the rock strength based on TBM parameters. It is noted that the establishment model of the rock strength σ_{ci} only concentrated on the Murree tertiary hard rocks or similar geological parameters, such as the brittle and higher-strength sandstone and grained grayish siltstone, which is highly correlated with the occurrence of rockbursts. The regression equation does not apply to the soft brown siltstone or mudstone.

5. Effectiveness of the novel rockburst criterion and typical cases study

An analysis of rockburst cases was carried out to verify the rationality and applicability of the novel rockburst criterion. Results obtained from the novel and traditional rockburst criteria were compared with the actual rockburst records gathered during the excavation of the NJ-TBM tunnel.

For the novel rockburst criterion, the test results of the in-situ stress are available in Table 2 and calculated with Eqs. (1)–(3). GSI is calculated with Eq. (16), based on TBM parameter of the boring/specific energy (SE). Similarly, the rock strength σ_{ci} is obtained rapidly using the TBM performance parameter FPI as per Eq. (18). Ultimately, the rockburst evaluation index is obtained by Eq. (9) and the rockburst grade is determined with Table 3. On the other hand, the traditional criteria e.g., Barton et al. (1974), Russenes (1974) can be obtained by

Table 6
Application of novel criteria to rockbursts.

Geological units	Chainage	Depth (m)	σ_1	σ_3	σ_{max}	σ_{ci}	GSI	Barton et al. (1974)		Russenes (1974)		New criterion		Site records of rockburst
								σ_{ci}/σ_1	Result	$\sigma_\theta/\sigma_{ci}$	Result	$\sigma'_{rm}/\sigma_{max}$	Result	
Massive sandstone (a drag fold with a thickened fold hinge against the fault)	09 + 700–09 + 671	1250	88.9	54.9	66.4	128.5–136.2	50.43	1.50	Intensive	1.80	Intensive	1.34–1.91	Intensive	Multiple ejection with big sound and overbreak continually (2 intensive rockburst)
	09 + 671–09 + 649	1300	88.9	54.9	60.35	130.3–137.5	53.94	1.48	Intensive	1.82	Intensive	1.51–2.43	Moderate-intensive	Multiple ejection with big sound and overbreak continually (1 intensive rockburst)
Massive sandstone	09 + 649–09 + 626	1365	54.9	52.2	51.75	137.9–141.6	53.87	2.55	Intensive	0.86	Intensive	2.75–3.73	Moderate	Multiple ejection with continually small sound above the shield and overbreak continually
Interbedded “sandstone + siltstone” layer	09 + 626–09 + 610	1410	54.9	52.2	50.86	126.2–140.8	52.0	2.46	Intensive	0.90	Intensive	2.53–3.46	Moderate	Occasionally ejection but overbreak continually
Interbedded “sandstone + siltstone” layer	08 + 893–08 + 815	1530	54.90	43.30	58.58	113.7–159	52.40	2.48	Intensive	0.76	Intensive	2.67–3.38	Moderate	Multiple ejection with continually sound above the shield and overbreak continually
Mudstone+ “thin siltstone” layer	08 + 815–08 + 765	1555	54.90	43.30	59.26	110.6–138.1	50.88	2.27	Intensive	0.88	Intensive	2.54–3.10	Moderate	No ejection but overbreak occasionally
Sandstone	08 + 765–08 + 738	1560	54.90	43.30	59.40	127.6–139.9	52.68	2.44	Intensive	0.87	Intensive	2.88–3.18	Moderate	Multiple ejection with light sound above the shield and overbreak occasionally
Siltstone+“ thin sandstone and mudstone” layer	08 + 738–08 + 676	1630	106.84	54.56	61.31	120.8–143.2	52.12	1.24	Intensive	1.87	Intensive	3.08–3.57	Moderate	Occasionally ejection but overbreak continually
Sandstone+“thin mudstone and siltstone” layer	08 + 676–08 + 658	1636	107.20	54.76	61.47	122–143.2	52.80	1.24	Intensive	1.88	Intensive	3.13–3.60	Moderate	No ejection but minor overbreak continually
Interbedded “sandstone + siltstone” layer	08 + 658–08 + 555	1660	108.65	55.57	62.13	116.3–178	52.80	1.35	Intensive	1.53	Intensive	3.02–3.90	Moderate	No ejection but minor overbreak continually
Mudstone	08 + 555–08 + 535	1690	110.45	56.58	62.94	109.6–146.1	52.38	1.16	Intensive	1.89	Intensive	2.88–3.59	Moderate	No ejection and overbreak
Sandstone+“thin mudstone and siltstone” layer	08 + 535–08 + 513	1700	111.05	56.92	63.22	129.5–146.1	54.61	1.24	Intensive	1.90	Intensive	3.33–3.70	Moderate	Multiple ejection with light sound above the shield and overbreak occasionally
Mudstone+ “thin siltstone” layer	08 + 513–08 + 478	1725	112.55	57.76	63.90	119.6–144.7	51.54	1.17	Intensive	1.95	Intensive	3.02–3.53	Moderate	No ejection and overbreak
Interbedded “sandstone + siltstone” layer	08 + 478–08 + 408	1750	114.06	58.61	64.58	121.4–152.2	51.68	1.20	Intensive	1.87	Intensive	3.06–3.60	Moderate	Multiple ejection with light sound above the shield and overbreak occasionally
Mudstone+ “thin siltstone” layer	08 + 408–08 + 380	1770	115.26	59.28	65.13	109.7–138.1	50.70	1.08	Intensive	2.08	Intensive	2.81–3.42	Moderate	No ejection but overbreak continually
Siltstone+“ thin sandstone and mudstone” layer	08 + 380–08 + 306	1800	117.06	60.29	65.95	116.6–164.5	51.31	1.20	Intensive	1.78	Intensive	2.95–3.68	Moderate	Multiple ejection with large sound in sandstone and overbreak occasionally in mudstone
Interbedded “sandstone + siltstone” layer	08 + 306–08 + 154	1830	118.86	61.30	66.77	122.3–200.6	56.22	1.36	Intensive	1.48	Intensive	3.24–4.24	Light – Moderate	Multiple ejection with light sound above the shield and overbreak continually
Siltstone+“ thin sandstone ” layer	08 + 154–08 + 109	1865	120.97	62.48	67.72	117–156.7	52.41	1.13	Intensive	1.92	Intensive	2.99–3.65	Moderate	Multiple ejection with light sound above the shield and overbreak occasionally
Siltstone+“ thin sandstone ” layer	08 + 109–08 + 089	1880	121.87	62.99	68.13	125.1–172.3	54.58	1.22	Intensive	1.76	Intensive	3.22–3.89	Moderate	No ejection but minor overbreak occasionally
Sandstone + thin siltstone and mudstone layer	08 + 089–08 + 066	1890	122.47	63.32	68.40	90–138.6	51.3	0.93	Intensive	2.20	Intensive	2.48–3.43	Moderate	Multiple ejection with continually sound above the shield and overbreak continually
Sandstone	08 + 066–08 + 057	1900	123.07	63.66	68.68	118–164.2	58.1	1.15	Intensive	1.86	Intensive	3.23–4.01	Light – Moderate	Occasionally ejection and overbreak
Interbedded “mudstone + siltstone” layer	08 + 057–08 + 047	1900	123.07	63.66	68.68	92.1–130.5	53.6	0.90	Intensive	2.35	Intensive	2.58–3.46	Moderate	No ejection but overbreak occasionally

(*continued on next page*)

Table 6 (*continued*)

Geological units	Chainage	Depth (m)	σ_1	σ_3	σ_{max}	σ_{ci}	GSI	Barton et al. (1974)		Russenes (1974)		New criterion		Site records of rockburst
								σ_{ci}/σ_1	Result	$\sigma_\theta/\sigma_{ci}$	Result	σ'_{m}/σ_{max}	Result	
Interbedded "sandstone + siltstone" layer	08 + 047–08 + 001	1900	123.07	63.66	68.68	115.4–189.2	61.3	1.24	Intensive	1.62	Intensive	3.31–4.43	Light – Moderate	multiple ejection with large sound and overbreak continually above the shield
Sandstone + thin siltstone layer	08 + 001–07 + 959	1900	123.07	63.66	68.68	122.1–191.2	57.6	1.27	Intensive	1.60	Intensive	3.28–4.22	Light – Moderate	multiple ejection with continually sound above the shield and overbreak occasionally
Interbedded " siltstone + sandstone" layer	07 + 959–07 + 856	1950	126.08	65.35	70.04	86.6–198.3	60.6	1.13	Intensive	1.58	Intensive	2.69–4.45	Light – Moderate	multiple ejection with continually sound above the shield and local overbreak continually
Siltstone + thin sandstone and mudstone	07 + 856–07 + 788	1950	126.08	65.35	70.04	90.6–184.8	57.1	1.09	Intensive	1.69	Intensive	2.65–4.12	Light – Moderate	Occasionally ejection with light sound and overbreak

calculating the strength-stress ratio (Table 1). The rockbursts that occurred in different geological units are analyzed with the novel and traditional criteria, and the results are summarized in Table 6.

Table 6 indicates that classifications using the three criteria for the rockbursts are different. The tunnel is under intensive rockburst risk with the traditional strength-stress ratio of 0.9–2.48 from Barton et al., 1974 (σ_{ci}/σ_1) and 0.76–2.35 from Russenes 1974 ($\sigma_\theta/\sigma_{ci}$). While based on in situ rockbursts records, most rockbursts were light-moderate and the intensive rockburst occurred rarely during tunnel excavation. This research effort indicates that prediction using the novel criteria for the rockbursts cases study is in agreement with that obtained from our database, even though the rockbursts occurred in different geological units.

6. Conclusions

In this study, various rockburst events observed and recorded during construction of the NJ-TBM tunnel were statistically analyzed. Considering the multiple factors influencing the likelihood and character of rockburst during construction and the limitations of traditional rockburst criteria, a series of detailed studies were carried out and the following conclusions were obtained:

(1) The traditional rockburst criteria are practical and convenient for design engineers to predict rockbursts. However, it is considered too conservative and simple to predict rockburst events in complex geological conditions. Conservation and unreliability applying the three traditional strength-stress ratio criteria in rockbursts of the NJ-TBM tunnel are observed. This indicates it is uncertain whether higher in situ stress will lead to higher-grade rockbursts. The occurrence of rockbursts is also highly correlated with the rockmass quality and construction characteristics during the construction phase.

(2) A novel rockburst criterion was presented utilizing the rockmass strength-stress ratio method, which is defined as the ratio between the rockmass strength based on the Hoek–Brown strength criterion and the maximum horizontal stress perpendicular to the tunnel axis. This criterion relates the key influencing factors on rockburst, such as the characteristics of the rockmass, the in situ stress, the geologic structure, and nearby construction disturbances.

(3) In practical application at the NJ-TBM tunnel, some attempts on quantitative models of the geological strength index (GSI) and rock uniaxial compressive strength (σ_{ci}) were made based on the specific energy (SE) and the field penetration index (FPI) from the TBM performance database, respectively. This makes it possible to conventionally evaluate Hoek–Brown rockmass strength.

(4) The observations and classification of 26 rockbursts cases in different geological units indicate that the novel criterion greatly enhanced the accuracy and applicability of rockburst prediction during the construction phase, through comparative analysis with the traditional criteria.

If the stress distribution state, rockmass quality, and construction characteristics can be effectively evaluated, the rockburst could be better determined by the suggested rockburst criterion. Obviously, this criterion should be further verified with other TBM engineering rockburst data. Additional data from other TBM tunnels may help to provide some useful conclusions and expand the range of application of the novel rockburst criterion presented in this paper.

Acknowledgements

This work was supported by the National Program on Key Basic Research Project (973 Program) (Grant Nos. 2015CB057906), the National Natural Science Foundation of China (Grant Nos. 51579238), and Youth Innovation Promotion Association CAS. In addition, authors

wish to thank CGGC Company and NEELUM-JHELUM CONSULTANTS in Pakistan, especially our colleagues for their help in the collection of required data.

References

Adoko, A.C., Gokceoglu, C., Wu, L., Zuo, Q.J., 2013. Knowledge-based and data-driven fuzzy modeling for rockburst prediction. Int. J. Rock Mech. Min. Sci. 61, 86–95.

Barton, N., Lien, R., Lunde, J., 1974. Engineering classification of rockmasses for the design of tunnel support. Int. J. Rock Mech. Min. Sci. 6 (4), 189–236.

Bawden, W.B., 2015. Neelum Jhelum Hydroelectric Project Rockburst Investigation Report.

Cai, M.F., 2016. Prediction and prevention of rockburst in metal mines – a case study of Sanshandao gold mine. J. Rock Mech. Geotech. Eng. 8 (2), 204–211.

Chen, B.R., Feng, X.T., Li, Q.P., Luo, R.Z., Li, S., 2015. Rock burst intensity classification based on the radiated energy with damage intensity at Jinping II Hydropower Station. China. Rock Mech. Rock. Eng. 48 (1), 289–303.

Code for geological survey of water resources and hydropower projects (GB50487-2008) [S]. Ministry of Construction of the PRC. Beijing: China Planning Press (in Chinese).

Goodman, R.E., 1980. Introduction to Rock Mechanics. Wiley, New York.

Gu, M.C., 2001. Research on rockburst in Qinling Railway Tunnel. Res. Water Resour. Hydropower 3 (4), 19–26 (in Chinese).

Hamidi, J.K., Shahriar, K., Rezai, B., et al., 2010. Performance prediction of hard rock TBM using Rockmass Rating (RMR) system. Tunn. Undergr. Space Technol. 25 (4), 333–345.

Hassanpour, J., Rostami, J., Khamehchiyan, M., Bruland, A., 2009. Development new equations for performance prediction. Geo Mech. Geoeng.: An Int. J. 4 (4), 287–297.

Hassanpour, J., Rostami, J., Zhao, J., 2011. A new hard rock TBM performance prediction model for project planning. Tunnel. Undergr. Space Technol. 26, 595–603.

He, M.C., Sousa, L.R., Miranda, T., Zhu, G., 2015. Rockburst laboratory tests database—application of data mining techniques. Eng. Geol. 185, 116–130.

Hedley, David, G.F., 1992. Rockburst Handbook for Ontario Hardrock Mines. Canmet.

Hoek, E., Brown, E.T., 1997. Practical estimates of rockmass strength. Int. J. Rock Mech. Min. Sci. Geo Mech. Abstr. 34 (8), 1165–1186.

Hoek, E., Brown, E.T., 1980. Underground Excavations in Rock. Institution of Mining and Metallurgy, London, pp. 527.

Hoek, E., Carranza-Torres, C., Corkum, B., 2002. Hoek-brown failure criterion-2002 edition. Proc. NARMS-Tac. 1, 267–273.

Hoek, E., Marinos, P., Benissi, M., 1998. Applicability of the Geological Strength Index (GSI) classification for very weak and sheared rockmasses. The case of the athens schist formation. Bull. Engg. Geol. Env. 57 (2), 151–160.

Jenkins, F.M., Williams, T.J., Wideman, C.J., 1990. Rock burst mechanism studies at the Lucky Friday Mine. In: Proc. 31st U.S. Symp. Rock Mechanics, WV Univ., Balkema, Rotterdam, pp. 955–962.

Kaiser, P.K., Cai, M., 2012. Design of rock support system under rockburst condition. J. Rock Mech. Geotech. Eng. 4 (3), 215–227.

Kaiser, P.K., Tannant, D.D., McCreath, D.R., 1996. Canadian Rockburst Support Handbook. eomechanics Research Centre, Laurentian University, Sudbury, Ontario.

Khan, E.A.K., 2012. Engineering of headrace tunnel for Neelum Jhelum hydropower project. Centenary Celebration (1912–2012), Paper No. 708.

Kidybiski, A., 1981. Bursting liability indices of coal. Int. J. Rock Mech. Min. Sci. Geomech. Abstr. 18 (4), 295–304.

Ma, T.H., Tang, C.A., Tang, L.X., Zhang, W.D., Wang, L., 2015. Rockburst characteristics and micro-seismic monitoring of deep-buried tunnels for Jinping II Hydropower Station. Tunn. Undergr. Space Technol. 49, 345–368.

Marinos, P., Hoek, E., 2000. GSI: a geologically friendly tool for rock mass strength estimation//ISRM International Symposium. International Society for Rock Mechanics.

Marinos, V., Marinos, P., Hoek, E., 2005. The geological strength index: applications and limitations. Bull. Eng. Geol. Environ. 64 (1), 55–65.

Nelson, P.P., O'Rourke, T.D., Kulhawy, F.H., 1983. Factors affecting TBM penetration rates in sedimentary rocks. In: 24th U.S. Symp. Rock Mech., pp. 227–237.

Russenes, B.F., 1974. Analysis of rock spalling for tunnels in steep valley sides (in Norwegian). M. Sc. thesis. Norwegian Institute of Technology, Dept. of Geology, pp. 247.

Sanio, H.P., 1985. Prediction of the performance of disc cutters in anisotropic rock. Int. J. Rock Mech. Min. Sci. Geomech. Abstr. 22 (3), 153–161.

Shang, Y.J., Zhang, J.J., Fu, B.J., 2013. Analyses of three parameters for strain mode rockburst and expression of rockburst potential. Chin. J. Rock Mech. Eng. 32, 1520–1527.

Sousa, L.R., 2012. Report for the State Administration of Foreign Experts Affairs. SKLGDUE, Beijing, pp. 54.

Stillea, H., Palmströmb, A., 2003. Classification as a tool in rock engineering. Tunnel. Undergr. Space Technol. 18 (4), 331–345.

Turchaninov, I.A., 1978. Interrelation between the stressed state of rocks and their properties. J. Min. Sci. 14 (2), 140–144.

Wang, C., Wu, A., Lu, H., Bao, T., Liu, X., 2015. Predicting rockburst tendency based on fuzzy matter–element model. Int. J. Rock Mech. Min. Sci. 75, 224–232.

Wang, C.H., Guo, Q.L., Ding, L.F., Liu, L.P., 2009. High in–situ stress criteria for engineering area and a case analysis. Rock and Soil Mechanics. 30 (8), 2359–2364 (in Chinese).

Wang, C.H., Guo, Q.L., Jia, L., 2011. Theoretical analysis of high stress criterion based on the Hoek-Brown criterion. Rock Soil Mech. 32 (11), 3325–3332 (in Chinese).

Zhang, J.J., Fu, B.J., Li, Z.K., Song, S.W., Shang, Y.J., 2012. Criterion and classification for strain mode rockbursts based on five-factor comprehensive method. In: Proceedings of the 12th ISRM International Congress on Rock Mechanics. Beijing, pp.1435–1440.